PERGAMON

www.elsevier.nl/locate/poly

Polyhedron 20 (2001) 363–372

POLYHEDRON

Synthesis, spectral characterization and electrochemical studies of mixed-ligand complexes of platinum(II) with 2-(arylazo)pyridines and catechols. Single-crystal X-ray structure of dichloro{2-(phenylazo) pyridine}platinum(II)

Goutam Kumar Rauth [a], Sanjib Pal [a], Debasis Das [a], Chittaranjan Sinha [a,*], Alexander M.Z. Slawin [b], J. Derek Woollins [b]

[a] *Department of Chemistry, The University of Burdwan, Burdwan 713104, India*
[b] *Department of Chemistry, University of St-Andrews, St. Andrews KY16 9ST, UK*

Received 23 May 2000; accepted 7 August 2000

Abstract

The reaction of 2-(arylazo)pyridines, $RH_4C_6N{=}NC_5H_4N$ (aap, **1** where R = H (pap), *p*-Me (*p*-tap), *p*-Cl (*p*-Clpap)) with K_2PtCl_4 in 1:2 boiling acetonitrile–water affords orange–red complexes of the type $Pt(aap)Cl_2$ (**2**). The IR spectrum shows two ν(Pt–Cl) stretches suggesting *cis*-$PtCl_2$ configuration. The structural confirmation was carried out by an X-ray diffraction study of $Pt(pap)Cl_2$ (**2a**). The addition of catechols to a chloroform–methanol solution of $Pt(aap)Cl_2$ in the presence of Et_3N yielded green colored mixed-ligand complexes of the formula Pt(aap)(*O*,*O*) (*O*,*O* = catecholate (cat) (**3**), 4-*tert*-butylcatecholate (tbcat), (**4**), 3,5-di-*tert*-butylcatecholate (dtbcat) (**5**) and tetrachlorocatecholate (tccat) (**6**)). The complexes were characterized by elemental analyses, IR, UV–Vis–NIR and ^{1}H NMR spectral data. Electronic spectra exhibit a ligand–ligand charge transfer (LLCT) transition at NIR region; the position and symmetry of the band depend on the type of substituent on the catechol frame. This is qualitatively assigned as $3b_1(cat) \rightarrow \pi^*(aap)$ transition. Cyclic voltammogram of the complexes show four successive redox responses: two couples positive to SCE are referred to as oxidation of catechol to semiquinone and semiquinone to quinone, respectively and two couples negative to SCE correspond to azo reductions.

Keywords: Azopyridine; Catechols; Platinum(II); Structure; Electrochemistry

1. Introduction

The π-acidity of the azoimine group, –N=N–C=N–, and its ability to stabilize low valent metal redox states has encouraged the study of its chemistry and molecular architecture design with this group [1–20]. 2-(Arylazo)pyridine (aap, **1**) is one such molecule whose coordination chemistry with transition metals has been extensively studied [3–18] and maximum effort has been given to explore the chemical activity of the platinum group metals [3–14]. However, platinum remains untouched. Much current research on platinum(II) with *N*-donor ligands is targeted to synthesize analogues of cisplatin [21,22]. The use of *N*,*N*-donor ligands instead of ammonia appeared favorable because of the thermodynamic stability of the chelate complexes. The π-acidity of the function, –N=N–C=N–, has manifested itself in [Pd(*N*,*N*)(*O*,*O*)] (where *N*,*N* = 2-(arylazo)pyridines; *O*,*O* = catecholates) in a ligand–ligand charge transfer transition (LLCT) [8]. The band position and symmetry depend on the substituents in the ligand frame and on the polarity of the solvent used [23–25]. Besides, platinum catecholates have been reported to have anticancer activity and are used as labels for the preparation of metalloantigens [26]. Transition metal complexes of catecholate and related ligands are of wide-ranging interest [27,28]. Herein we account the synthesis, spectral characterization and electrochemical properties of 2-(arylazo)-pyridine complexes of platinu-

* Corresponding author. Tel.: +91-342-57-683; fax: +91-342-64-452.
E-mail address: c-r-sinha@yahoo.com (C. Sinha).

0277-5387/01/$ - see front matter
PII: S0277-5387(00)00530-1

m(II) and their catecholato derivatives. The structure of dichloro-(2-(phenylazo)pyridine)platinum(II) is supported by X-ray crystallography.

2. Experimental

2.1. Materials

$H_2PtCl_6{\cdot}xH_2O$ was purchased from Arrora Mathey, Calcutta, India. K_2PtCl_4 was prepared from H_2PtCl_6 following the reported method [29]. 2-(Arylazo)pyridines (aap) were synthesized according to the published procedure [8]. Pyrocatechol (H_2cat), 3,5-di-*tert*-butylcatechol (H_2dtbcat), tetrachlorocatechol (H_2tccat) were obtained from Aldrich. 4-*tert*-Butylcatechol (H_2tbcat) was a product of Fluka. Catechols were purified by recrystallization from benzene. Dichloromethane and acetonitrile were further purified by distillation over P_4O_{10}. Tetrabutylammonium perchlorate (n-Bu_4NClO_4) was prepared and recrystallized by a previously reported method [23]. Nitrogen gas was purified by successive bubbling through alkaline pyrogallol solution and concentrated sulfuric acid. Commercial grade SRL silica gel (60–120 mesh) was used for column chromatography. Triethylamine, hydrazinesulfate and all other chemicals and solvents used in preparative work were of reagent grade and were used as received.

2.2. Instrumentation

Microanalytical data (C, H, N) were collected using a Perkin–Elmer 2400 CHNS/O elemental analyzer. Spectroscopic data were obtained using the following instruments: UV–Vis–NIR spectra, Shimadzu UV 160 A and Hitachi 330; IR spectra (KBr disk, 4000–200 cm^{-1}), FTIR JASCO model 420; ^1H NMR from Brucker AC(F) 300 MHz FT NMR spectrometer. Electrochemical measurements were carried out using computer-controlled PAR model 270 VERSASTAT electrochemical instruments with a GC milli-electrode. All measurements were carried out under dinitrogen environment at 298 K with reference to a saturated calomel electrode (SCE) in acetonitrile. The reported potentials are uncorrected for junction potential.

2.3. Preparation of complexes

2.3.1. Dichloro-{2-(phenylazo)pyridine}platinum(II), Pt(pap)Cl_2 (**2a**)

To a nitrogen flushed solution of K_2PtCl_4 (0.22 g, 0.53 mmol) in water (20 ml) under refluxing conditions was added 2-(phenylazo)pyridine (0.1 g, 0.55 mmol) in MeCN (10 ml). The reaction was continued for 24 h and cooled to room temperature (r.t.). The brown–red solution was evaporated in a steam bath and the solution was reduced to half of its original volume. The dark precipitate was filtered and washed with hot water and finally with cold 1:1 MeCN–H_2O (v/v). It was then dried over $CaCl_2$. The product was then dissolved in a minimum volume of CH_2Cl_2 and was chromatographed on silica gel column (30 × 1 cm). A deep orange–red band eluted using 3:1 C_6H_6–MeCN (v/v). Crystals were obtained by complete evaporation of the eluted solution at r.t. The yield was 0.17 g (74%). Pt(*p*-tap)Cl_2 and Pt(*p*-Clpap)Cl_2 were prepared following an identical procedure and the yields were 68 and 79%, respectively.

2.3.2. Preparation of catecholato-(2-(phenylazo)pyridine)platinum(II), [Pt(pap)(cat)] (**3a**)

Pt(pap)Cl_2, (0.325 g, 0.72 mmol) was dissolved in $CHCl_3$ (15 cm^3) and the solution was degassed by bubbling N_2. To this solution pyrocatechol (0.085 g, 0.77 mmol) in MeOH (10 cm^3) was slowly added followed by triethylamine (2 mmol) under N_2. The solution was stirred for 1 h and the color changed from orange–red to green. The solution volume was reduced to one-third of its original volume by N_2 bubbling and the dark green precipitate that formed was filtered, washed with MeOH and dried over $CaCl_2$. The dried mass was dissolved in a minimum volume of CH_2Cl_2, chromatographed over silica gel and the desired green band was eluted by 3:2 C_6H_6–MeCN (v/v). Evaporation of the solvent in vacuo afforded the pure crystalline product. The yield was 0.28 g (58%). All other complexes were prepared by an identical procedure and the yields varied in the range 45–72%.

2.4. X-ray crystal structure and analysis

A crystal of Pt(pap)Cl_2 suitable for X-ray work was grown by slow diffusion of hexane into a dichloromethane solution at 298 K. The crystal size was $0.1 \times 0.1 \times 0.3$ mm^3. Data were collected on a Siemens SMART CCD diffractometer with graphite monochromatized Mo Kα radiation ($\lambda = 0.71073$ Å) at 295 K. Data for the crystal and the collection parameters are listed in Table 1. The data were corrected for absorption effects by an empirical method using azimuthal scan data. Systematic absences led to the identification of the space group as monoclinic $C2/c$. Of the 22 453 reflections collected, 8751 with $I > 2\sigma(I)$ were used for structure solution. The structure was solved by the conventional heavy atom method and was refined by the full-matrix least-square method on all F_o^2 data using the SHELXTL 5.03 package on a Silicon Graphics Indigo-R4000 [20]. Hydrogen atoms were included in calculated positions and refined with isotropic thermal parameters.

Table 1
Summarized crystallographic data for Pt(pap)Cl_2

Empirical formula	$C_{11}H_9Cl_2N_3Pt$
Formula weight	449.20
Crystal system	monoclinic
Space group	$C2/c$
a (Å)	56.0852(9)
b (Å)	9.42210(10)
c (Å)	14.3708(2)
β (°)	99.9230(10)
V (Å^3)	7480.5(2)
Z	24
T (K)	295
D_{calc} (Mg m^{-3})	2.393
μ(Mo Kα) (mm^{-1})	11.661
Transmission coefficient [a]	0.368
Parameters refined	461
R [b]	0.0348
wR [c]	0.0687
Goodness-of-fit [d]	0.878

[a] Maximum value normalized to 1.
[b] $R = \Sigma|F_o - F_c|/\Sigma F_o$.
[c] $wR = [\Sigma w(F_o^2 - F_c^2)/\Sigma wF_o^4]^{1/2}$; $w = 1/[\sigma^2(F_o^2) + (0.0473P)^2 + 14.3394P]$, $P = (F_o^2 + 2F_c^2)/3$.
[d] Goodness of fit is defined as $[w(F_o - F_c)/(n_o - n_v)]^{1/2}$ where n_o and n_v denote the numbers of data and variables, respectively.

3. Results and discussion

3.1. Synthesis

The arylazopyridines (aap) and platinum(II) complexes described in this work along with the methods used for their preparation are shown in Scheme 1. The arylazopyridines were obtained by the condensation of nitrosoaromatics with 2-aminopyridine [8]. They reacted with K_2PtCl_4 in acetonitrile–water solution under refluxing conditions affording orange–red Pt(aap)Cl_2 (**2**) in high yields. Addition of Et_3N to solutions of **2** and catechols in $CHCl_3$–MeOH under N_2 immediately changed the color from orange to brown–green and the products separated on slow bubbling of N_2 for a period of 1 h or more. Removal of the solvents followed by chromatographic purification afforded the catecholato complexes [Pt(*N*,*N*)(*O*,*O*)] (**3**–**6**) in high yield. The complexes are nonconducting and ESR silent. The compositions of the complexes are supported by microanalytical data (Table 2).

3.2. Single-crystal X-ray structure of Pt(pap)Cl_2

An X-ray quality single crystal is obtained by slow diffusion of dichloromethane solution into hexane. The asymmetric unit of the crystal lattice constituted of these molecules and is structurally comparable with dichloro{2-(phenylazo)pyridine}palladium(II) [30]. A view of the triad including the atom numbering scheme is shown Fig. 1 and selected bond parameters are listed in Table 3. In terms of bond distances, angles, as well as gross geometry, the three molecules are closely akin to one another. Some common features are as follows: the PtN_2Cl_2 coordination sphere is a good plane with no atom deviating > 0.045 Å from the mean plane. The dimensions of the chelate ring compare well with those in other structurally characterized chelates of this ligand [3,31]. The average chelate bite angle is 78.1(3)° and is considerably deviated from the ideal square planar values. The average Cl–Pt–Cl angle is approximately 89.3°. The pendant phenyl ring is planar and inclined at an acute angle with the chelate ring (lies between 42–48°).

The average Pt–N(azo) and Pt–N(Py) distances are approximately 1.988 and 2.010 Å, respectively. The shortening of the Pt–N (azo) distance may be due to significant back bonding between t_2(Pt) and π*(pap)

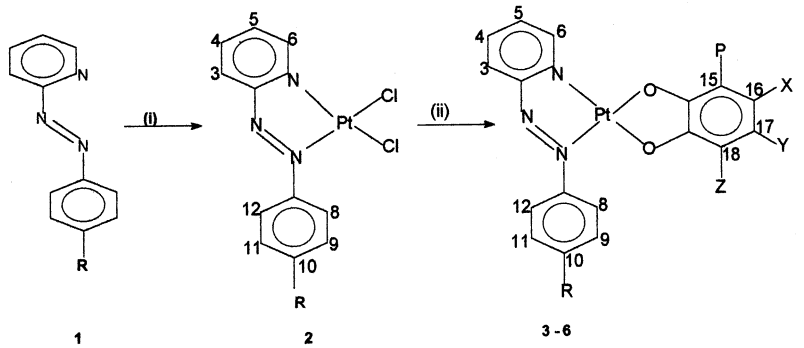

R= H (pap), Me(*p*-tap), Cl(*p*-Clpap)

	3	4	5	6
P	H	H	Bu^t	Cl
X	H	Bu^t	H	Cl
Y	H	H	Bu^t	Cl
Z	H	H	H	Cl

Scheme 1. (i) K_2PtCl_4 in 1:2 MeCN–H_2O (v/v) reflux, 24 h; (ii) catechols, Et_3N in $CHCl_3$–MeOH stir under N_2 atmosphere, 8 h.

Table 2
Microanalytical [a], IR [b] and UV–Vis [c] spectral data

Compound	Elemental analyses (%)			Infrared data (cm^{-1})			UV–Vis spectral data λ_{max} (nm^{-1}) (ε (mol^{-1} cm^{-1})
	C	H	N	ν(N=N)	ν(Pt–Cl)	ν(Pt–O)	
Pt(pap)Cl_2	29.31 (29.39)	1.92 (2.00)	9.44 (9.35)	1385	324, 345		493(2240), 407(7011) 383(8537)
Pt(*p*-tap)Cl_2	31.17 (31.09)	2.31 (2.37)	9.12 (9.06)	1390	318, 340		489(2968), 412(11,482) 391(10,968)
Pt(*p*-*C*lpap)Cl_2	27.38 (27.29)	1.71 (1.65)	8.58 (8.68)	1383	315, 340		493(1940), 385(9743) 367(9090)
Pt(pap)(cat)	42.05 (41.96)	2.73 (2.67)	8.57 (8.64)	1358		570	870(2300), 646(1800) 384(9090)
Pt(pap)(tbcat)	46.80 (46.48)	3.91 (3.87)	7.54 (7.75)	1350		590	937(4619), 652(1776) 386(9000)
Pt(pap)(dtbcat)	50.50 (50.16)	4.84 (4.85)	7.10 (7.02)	1350		590	1011(5397), 749(2936) 390(7865)
Pt(pap)(tccat)	32.60 (32.68)	1.50 (1.44)	6.79 (6.73)	1360		580	759(4385), 609(3141) 384(12732)
Pt(*p*-tap)(cat)	43.09 (43.19)	3.08 (2.99)	8.47 (8.40)	1355		580	857(8191), 632(2065) 401(14647)
Pt(*p*-tap)(tbcat)	47.41 (47.47)	4.20 (4.14)	7.63 (7.55)	1350		595	895(5320), 694(5519) 409(15460)
Pt(*p*-tap)(dtbcat)	51.04 (50.97)	5.00 (5.06)	6.95 (6.86)	1355		600	988(9977), 672(1842) 402(12639)
Pt(*p*-tap)(tccat)	33.78 (33.85)	1.81 (1.72)	6.64 (6.58)	1365		575	750(5323), 605(2244) 415(11055)
Pt(*p*-*C*lpap)(cat)	39.07 (39.18)	2.40 (2.31)	8.00 (8.07)	1360		580	893(3208), 642(2675) 392(17800)
Pt(*p*-*C*lpap)(tbcat)	43.66 (43.70)	3.54 (3.47)	7.35 (7.28)	1365		585	989(4619), 672(1211) 391(7021)
Pt(*p*-*C*lpap)(dtbcat)	47.50 (47.42)	4.80 (4.43)	6.68 (6.64)	1365		580	1090(2730), 799(6594) 400(18200)
Pt(*p*-*C*lpap)(tccat)	31.00 (30.97)	1.18 (1.21)	6.45 (6.38)	1355		600	766(1240), 513(853), 398(6094)

[a] Calculated values are in parenthesis.
[b] In KBr disk.
[c] In CH_2Cl_2.

orbitals. The N=N distance (average approximately 1.273 Å) is comparable with other reported values [3,31]. A packing view down to the *a*-axis suggests two molecular units (Pt(1) and Pt(3)) in the triad are closely associated and the Pt–Pt distance is approximately 3.6 Å.

The difference between the three molecules lies primarily in the details of conformation. The pendent phenyl ring is inclined differently: molecule 1, 42.4°; molecule 2, 48.2°; molecule 3, 45.2°. Pt deviates from the square plane, N_2Cl_2 by 0.036 Å (molecule **1**), 0.028 Å (molecule **2**) and 0.020 Å (molecule 3). Torsion angles also vary in a characteristic manner. Examples from those among the atoms of the chelate ring are given below. The three molecules represent an unusual and subtle form of conformational isomerism in a metal chelate sustained by the crystal lattice.

N(7)–Pt(1)–N(1)–C(2)	8.4	Pt(I)–N(I)–C(2)–N(2)	−10.0
N(27)–Pt(2)–N(21)–C(22)	−3.7	Pt(2)–N(2I)–C(22)–N(22)	3.6
N(47)–Pt(3)–N(41)–C(42)	2.5	Pt(3)–N(4I)–C(42)–N(42)	−3.0
N(1)–Pt(1)–N(7)–N(2)	−6.4	Pt(1)–N(7)–N(2)–C(2)	2.9
N(21)–Pt(2)–N(27)–N(22)	3.9	Pt(2)–N(27)–N(22)–C(22)	−3.0
N(41)–Pt(3)–N(47)–N(42)	−2.0	Pt(3)–N(47)–N(42)–C(42)	0.9

Table 3
Selected bond distances (Å) and bond angles (°)

Distances		Angles	
Molecule 1			
Pt(1)–N(1)	2.012(6)	N(1)–Pt(1)–N(7)	77.8(3)
Pt(1)–N(7)	1.997(6)	Cl(1)–Pt(1)–Cl(2)	89.33(8)
Pt(1)–Cl(1)	2.292(2)	N(1)–Pt(1)–Cl(2)	173.7(2)
Pt(1)–Cl(2)	2.303(2)	N(7)–Pt(1)–Cl(1)	172.8(2)
Pt(2)–N(7)	1.284(8)	N(1)–Pt(1)–Cl(1)	95.0(2)
		N(7)–Pt(1)–Cl(2)	97.9(2)
Molecule 2			
Pt(2)–N(2)	2.006(7)	N(21)–Pt(2)–N(27)	78.2(3)
Pt(2)–N(27)	1.987(7)	Cl(3)–Pt(2)–Cl(4)	89.50(9)
Pt(2)–Cl(3)	2.303(2)	N(21)–Pt(2)–Cl(4)	176.0(2)
Pt(2)–Cl(4)	2.297(2)	N(27)–Pt(2)–Cl(3)	172.3(2)
Pt(22)–N(27)	1.267(9)	N(21)–Pt(2)–Cl(3)	94.3(2)
		N(27)–Pt(2)–Cl(4)	97.9(2)
Molecule 3			
Pt(3)–N(41)	2.011(6)	N(41)–Pt(3)–N(47)	78.3(3)
Pt(3)–N(47)	1.985(6)	Cl(5)–Pt(3)–Cl(6)	89.05(8)
Pt(3)–Cl(5)	2.293(2)	N(41)–Pt(3)–Cl(6)	174.4(2)
Pt(3)–Cl(6)	2.299(2)	N(47)–Pt(3)–Cl(5)	172.8(2)
N(42)–N(47)	1.268(8)	N(41)–Pt(3)–Cl(5)	94.8(2)
		N(47)–Pt(3)–Cl(6)	98.0(2)

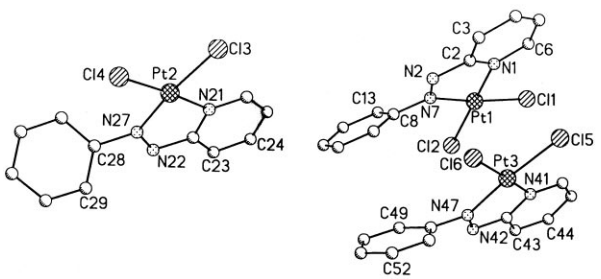

Fig. 1. Plot of Pt(pap)Cl_2 with 50% probability and atom labeling pattern.

3.3. Spectral studies

The IR spectra of Pt(aap)Cl_2 (**2**) exhibit a sharp single stretch at approximately 1385 cm^{-1} correspond to ν(N=N) which is lowered by 40 cm^{-1} from that of the free ligand value [15] (approximately 1425 cm^{-1}). In catecholato complexes, Pt(aap)(*O*,*O*) (**3**–**6**), the ν(N=N) appears at (Table 2) approximately 1355 cm^{-1}. The lowering of the frequency may attribute to the extensive $d(Pt) \rightarrow \pi^8(aap)$ back bonding or $3b_1(cat) \rightarrow \pi^8(aap)$ [8,24] in the catecholato complexes. The ν(N=N) in the present complexes appear at lower energy compared to the analogous Pd(aap)(*O*,*O*) complexes [8] (approximately 1375 cm^{-1}) which is corroborated by the general trend in periodic properties [32] of Pd and Pt. The *cis*-$PtCl_2$ configuration of Pt(aap)Cl_2 is established by the appearance of two distinct Pt–Cl stretching bands at 315 and 340 cm^{-1} which are absent in the catecholato complexes (Table 2). This confirms the nucleophilic displacement of Pt–Cl and the appearance of a new band around 450–500 cm^{-1} attributable to a Pt–O stretch suggests catecholato binding. On comparing the spectra of Pt(aap)Cl_2 and Pt(aap)(*O*,*O*) an additional band at 1250–1280 cm^{-1} was observed. This corresponds to the C–O stretching vibration of catechols. A strong band near 1400–1480 cm^{-1} in Pt(aap)(*O*,*O*) is also observed but this region of the spectrum is complicated by vibrations from azopyridines.

The solution electronic spectra of the complexes were recorded in dichloromethane. Pt(aap)Cl_2 (**2**) exhibits absorptions at around 490 and 400 nm and the absorptions below 400 nm are not considered as they correspond to intraligand charge transfer transitions. The absorption spectra of catecholato complexes, Pt(aap)(*O*,*O*), are different from their parent complexes (Fig. 2, Table 2). The most significant feature of the spectrum is the appearance of new band in the red to near-IR region. The position of the band is highly dependent on the nature of the substituent(s) in the catechol and azopyridine fragments [8,23,24]. This band is assigned as a ligand-to-ligand charge transfer (LLCT) transition involving the HOMO of catechol and the LUMO of arylazopyridine or the redox orbitals constituted by platinum(II) and arylazopyridine. The observed trend in the wavelength of the band maxima for a particular catechol is *p*-Clpap > pap > *p*-*t*ap. The trend of the band maxima for a particular azopyridine fragment is dtbcat > tbcat > cat > tccat. The HOMO of dtbcat is expected to have the highest energy in the series because of the electron releasing effect of two Bu^t groups. In the tccat complex, the HOMO has lower energy than the corresponding cat because of the electron withdrawing character of Cl groups. In *p*-Clpap the energy of the π^* orbital (LUMO) is of lower value compared to pap because of the electron withdrawing effect of Cl groups and the reverse is true of *p*-tap for the inductive effect of the –Me group. Thus the LLCT band is qualitatively described [33] as a $3b_1(cat) \rightarrow \pi^*(aap)$ charge transfer transition.

The stereochemistry of Pt(aap)Cl_2 (**2**) and [Pt(aap-(*O*,*O*)] (**3**–**6**) is supported by ^{1}H NMR spectral data. The ^{1}H NMR spectra of the complexes were recorded in $CDCl_3$ at 298(2) K. The atom numbering pattern of complexes is as shown in Scheme 1 and the spec-

tral data are collected in Table 4. Pyridine protons (3H–6H) appear in the downfield region relative to the azoaryl protons (8H–12H). The aryl protons move in an usual manner [8] with the substituents in the ring. In catecholato complexes [Pt(aap)(*O*,*O*)] (**3**–**6**) these signals experience an upfield shift compared with the parent compound $Pt(aap)Cl_2$ (**2**). This may be due to better charge transfer from the catecholato group to platinum(II) than the chloride ions or more back-bonding from the metal d-orbitals to the π*(aap) compared with chloride. The resonance of 6H exhibits coupling with ^{195}Pt ($I = 1/2$, abundance 33.7%) and the coupling constant $^{3}J_{Pt-H}$ is 20–30 Hz (Fig. 3). The protons of the catecholato ring appear upfield relative to the arylazopyridine signals which is expected in view of the electron releasing effect of the catecholato oxygen atoms. The complexes [Pt(aap)(cat)] (**3**) give a characteristic AA′BB′ pattern, while signals in the aliphatic region (δ; 1.3, 1.6 ppm) for [Pt(aap)(tbcat)] (**4**)/[Pt(aap)(dtbcat)] (**5**) are due to Bu^t protons. Complex **4** exhibits a singlet and two doublets in the upfield region assigned to 15H and 17,18H of tbcat, respectively. Complexes **4** and **5** exhibit slight downfield shifting of the catecholato protons (15H and 18H for **4** and 16H and 18H for **5**) although the electron releasing Bu^t group should show the reverse effect. The presence of a Bu^t group in the catechol ring (tbcat, dtbcat) increases the energy of the HOMO ($3b_1$) and induces increased charge transfer to the LUMO (π*) of the azopyridine compared to cat in [Pt(aap)(*O*,*O*)]. This may be the reason for the downfield shift of protons in tbcat and dtbcat relative to cat as well as the upfield shift of arylazopyridine protons in the complexes.

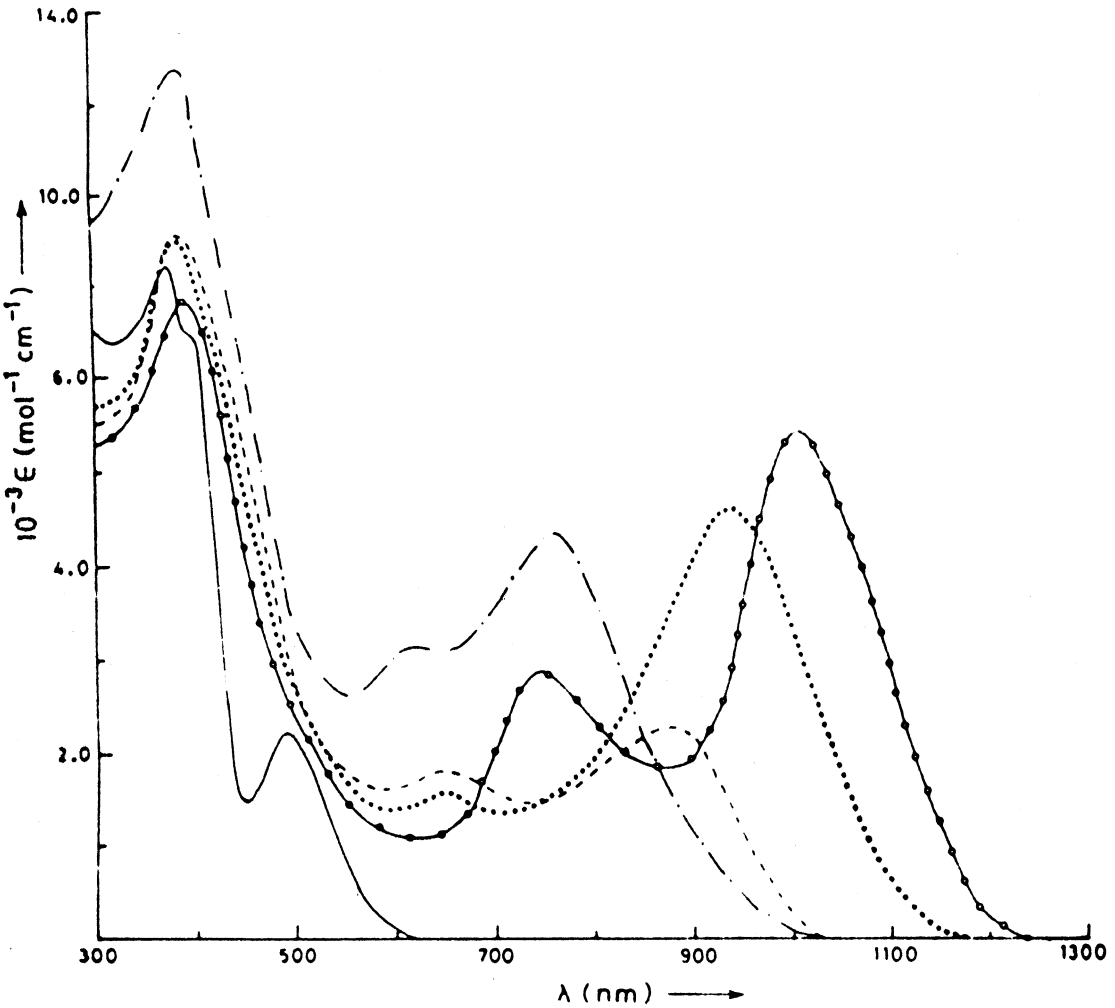

Fig. 2. Spectra of $[Pt(pap)Cl_2]$(—), [Pt(pap)(cat)](- - -), [PT(pap)(tbcat)](···), [Pt(pap)(dtbcat)](— ○ — ○ —) and [Pt(pap)(tccat)](— - —) in CH_2CL_2 at 298 K.

Table 4
^{1}H NMR spectral data [a]

Compound	δ, ppm (J, Hz)											
	3-H [b]	4-H [c]	5-H [c]	6-H [b e]	8,12-H [b]	9,11-H	10-H	15-H	16-H	17-H	18-H	R	Bu^t
Pt(pap)Cl_2	8.92	8.30	8.66	9.55	7.82	7.68 [f]	7.68 [f]						
	(8.0)	(8.0)	(8.0)	(7.0)	(7.4)								
Pt(p-tap)Cl_2	8.86	8.08	8.58	9.51	7.70	7.38							
	(8.0)	(7.8)	(7.8)	(7.0)	(8.0)	(8.0)							
Pt(p-Clpap)Cl_2	8.98	8.38	8.70	9.65	7.91	7.82							
	(8.0)	(8.0)	(8.0)	(7.0)	(8.0)	(8.0)							
Pt(pap)(cat)	8.61	8.04	7.61	9.31	7.75	7.56 [f]	7.56 [f]	6.60 [b]	7.11 [c]	7.10 [c]	6.60 [b]		
	(9.64)	(8.00)	(8.00)	(7.6)	(7.8)			(9.0)	(10.0)	(10.0)	(9.0)		
Pt(pap)(tbcat)	8.57	8.00	7.58	9.29	7.73	7.54 [f]	7.54 [f]	6.93 [d]		6.63 [b]	7.06 [b]		1.39
	(8.80)	(7.8)	(8.0)	(7.4)	(8.0)					(8.0)	(9.0)		
Pt(pap)(dtbcat)	8.55	7.97	7.55	9.22	7.67	7.52 [f]	7.52 [f]		6.68 [d]		7.11 [d]		1.35
	(7.8)	(9.0)	(9.0)	(7.22)	(8.0)								1.61
Pt(pap)(tccat)	8.64	8.00	7.62	9.33	7.67	7.58 [f]	7.58 [f]						
	(8.0)	(9.0)	(9.0)	(7.0)	(8.0)								
Pt(p-tap)(cat)	8.22	8.00	7.58	9.33	7.50	7.39 [b]		6.57 [b]	7.05 [c]	7.05 [c]	6.57 [c]	2.44	
	(8.4)	(8.0)	(8.0)	(7.4)	(8.4)	(8.0)		(9.0)	(10.0)	(10.0)	(9.0)		
Pt(p-tap)(tbcat)	8.50	8.02	7.55	9.30	7.46	7.39 [b]		6.90 [d]		6.61 [b]	7.03 [b]	2.40	1.38
	(8.0)	(8.0)	(8.0)	(7.8)	(8.0)	(8.0)				(9.0)	(9.0)		
Pt(p-tap)(dtbcat)	8.47	8.09	7.51	9.32	7.44	7.38 [b]			6.65 [d]		7.06 [d]	2.40	1.33
	(8.4)	(8.0)	(8.0)	(7.8)	(8.0)	(8.4)							1.54
Pt(p-tap)(tccat)	8.57	8.04	7.61	9.37	7.52	7.44 [b]						2.48	
	(8.0)	(8.0)	(8.0)	(7.0)	(9.0)	(8.0)							
Pt(p-Clpap)(cat)	8.65	9.09	7.63	9.35	7.50	7.64 [b]		6.56 [b]	6.98 [c]	6.91 [c]	6.56 [b]		
	(8.0)	(9.0)	(9.0)	(7.0)	(8.0)	(8.0)		(13.0)	(9.0)	(9.0)	(13.0)		
Pt(p-Clpap)(tbcat)	8.61	8.05	7.62	9.31	7.50	7.60 [b]		6.95 [d]		6.67 [b]	7.06 [b]		1.40
	(8.4)	(8.4)	(8.0)	(7.4)	(8.0)	(9.0)				(11.0)	(11.0)		
Pt(p-Clpap)(dtbcat)	8.58	8.00	7.58	9.30	7.48	7.61 [b]			6.70 [d]	7.11 [d]			1.35, 1.61
	(8.0)	(8.12)	(8.0)	(7.0)	(8.4)	(9.0)							
Pt(p-Clpap)(tccat)	8.68	8.04	7.65	9.36	7.52	7.62 [b]							
	(8.0)	(8.0)	(8.0)	(7.0)	(9.0)	(8.0)							

[a] In $CDCl_3$ using TMS as internal standard.
[b] Doublet.
[c] Triplet.
[d] Singlet.
[e] $^3J(^{195}Pt–H) = 20–30$ Hz.
[f] Multiplet.

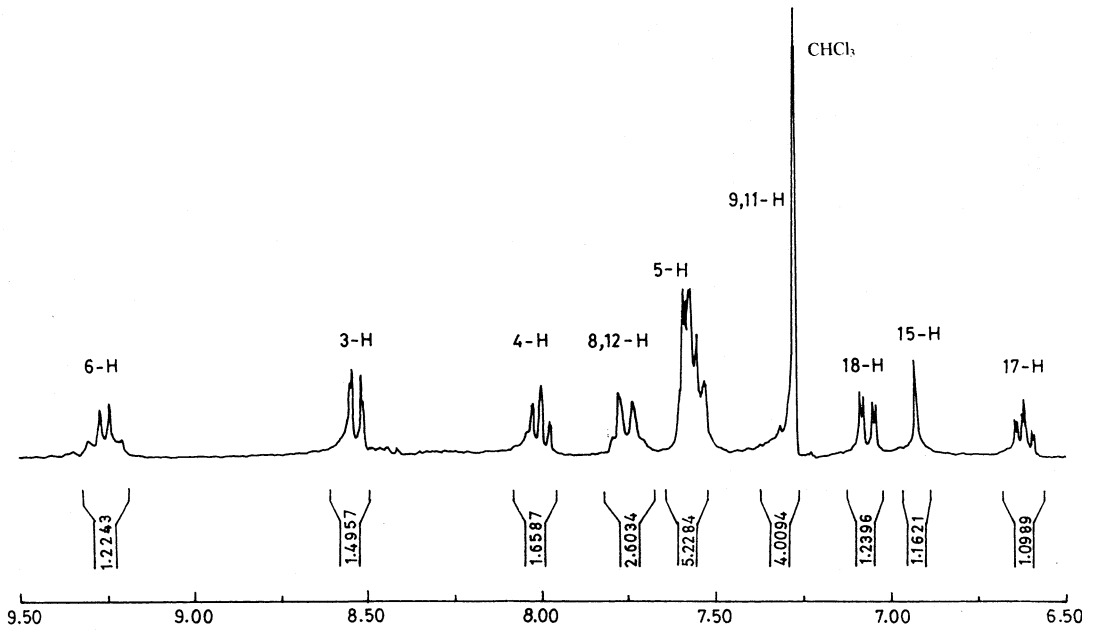

Fig. 3. Spectrum of [Pt(pap)(tbcat)] in $CDCL_3$ (300 MHz).

4. Redox studies

The redox properties of the complexes according to cyclic voltammetry are summarized in Table 5. All measurements were carried out with the use of a GC-working electrode in acetonitrile solution under a dinitrogen environment. All potentials are referenced to the saturated calomel electrode (SCE) in the presence of tetrabutylammonium perchlorate (n-Bu_4NClO_4) as supporting electrolyte. Pt(aap)Cl_2 exhibits only two responses at negative potential to SCE and Pt(aap)(O,O) gives four successive redox processes (Fig. 4) within the potential range $+1.5$ to -1.5 V versus SCE. The two couples at negative potential to SCE are due to azo reduction. The LUMO of aap can simultaneously accommodate two electrons. Since, this orbital has a large azo character, the reduction occurs at the azo center and is not considered further.

The anodic responses are due to the coordinated catechol oxidation (Eq. (1)) and the compounds undergo two successive one-electron redox processes with varying degrees of reversibility depending upon the type of substitutents present in the catecholato ring. The electron-donating catechols (tbcat, dtbcat) first give a reversible oxidation couple (Rcq/Rsq) followed by a second quasireversible couple (Rsq/Rq) while electron-withdrawing catechol (tccat) only gives a response of for an irreversible pattern. The redox data in Table 5 suggests that the potential (E_{pa}) is shifted to more positive values as the substitutent(s) in the bound catechol ring becomes more electron withdrawing.

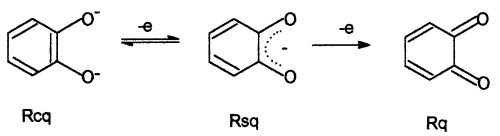

(1)

This is because the oxidation will be thermodynamically more facile when electron density flows into the catechol ring leading to stabilization of the positive charge of the cation radical [8,34]. The potentials of the first reduction and oxidation can qualitatively be related to the nature of the orbitals in these redox processes. These orbitals are involved in the CT transitions as $3b_1(cat) \rightarrow \pi^*(aap)$ [33].

5. Conclusion

The paper describes the synthesis of dichloro-{2-(arylazo)pyridine}platinum(II), Pt(aap)Cl_2 (**2**). The X-ray diffraction study has established the structure of the complex and suggests that the asymmetric unit of the crystal lattice consists of three molecules. Nucleophilic substitution of a *cis*-$PtCl_2$ motif by catechols (O,O) in the presence of Et_3N resulted in the synthesis of (catecholato){2 - (arylazo) - pyridine}platinum(II), [Pt(aap)-(O,O)] complexes (**3**–**6**). The absorption spectra of catecholato complexes exhibit significant differences from the dichloro complex in the red to near-IR region. The band is assigned to ligand–ligand charge transfer transition (LLCT). The absorption maxima are red shifted upon increasing the electron density on the

Table 5
Cyclic voltammetric data [a]

Compound	Catechol centered oxidation		aap-centered reduction	
	Rcq/Rsq $E^1_{1/2}$ (ΔE_p [b])	Rsq/Rq $E^2_{1/2}$ (ΔE_p [b])	aap^{2-}/aap^- $-E^3_{1/2}$ (ΔE_p [b])	aap^-/aap $-E^4_{pc}$
Pt(pap)Cl_2			0.14 (110)	1.12
Pt(*p*-tap)Cl_2			0.24 (90)	1.28
Pt(*p*-Clpap)Cl_2			0.14 (100)	1.07
Pt(pap)(cat)	0.68 (90)	1.10 (170)	0.42 (100)	1.25
Pt(pap)(tbcat)	0.55 (70)	1.02 (140)	0.48 (80)	1.38
Pt(pap)(dtbcat)	0.47 (80)	0.90 (120)	0.55 (80)	1.48
Pt(pap)(tccat)	1.04 [c]	1.51 [c]	0.33 (110)	1.18
Pt(*p*-tap)(cat)	0.62 (100)	1.05 (175)	0.46 (110)	1.28
Pt(*p*-tap)(tbcat)	0.52 (90)	0.96 (130)	0.54 (70)	1.41
Pt(*p*-tap)(dtbcat)	0.40 (100)	0.87 (110)	0.59 (85)	1.50
Pt(*p*-tap)(tccat)	1.00 (120)	1.43 [c]	0.38 (80)	1.21
Pt(*p*-Clpap)(cat)	0.74 (90)	1.23 [c]	0.39 (100)	1.22
Pt(*p*-Clpap)(tbcat)	0.59 (80)	1.08 (130)	0.43 (100)	1.33
Pt(*p*-Clpap)(dtbcat)	0.51 (80)	0.95 (130)	0.51 (100)	1.43
Pt(*p*-Clpap)(tccat)	1.06 (120)	1.58 [c]	0.31 (90)	1.15

[a] Solvent: 1:1 MeCN–$CHCl_2$ (v/v); supporting electrolyte *n*-Bu_4CLO_4; electrode GC milli-electrode; solute concentration 10^{-3} M; scan rate 50 mV s^{-1}; potentials are in volts vs. SCE.
[b] $\Delta E_p = (E_{pa} - E_{pc})$ in milivolts, where E_{pa} and E_{pc} are anodic and cathodic peak potentials.
[c] E_{pa}.

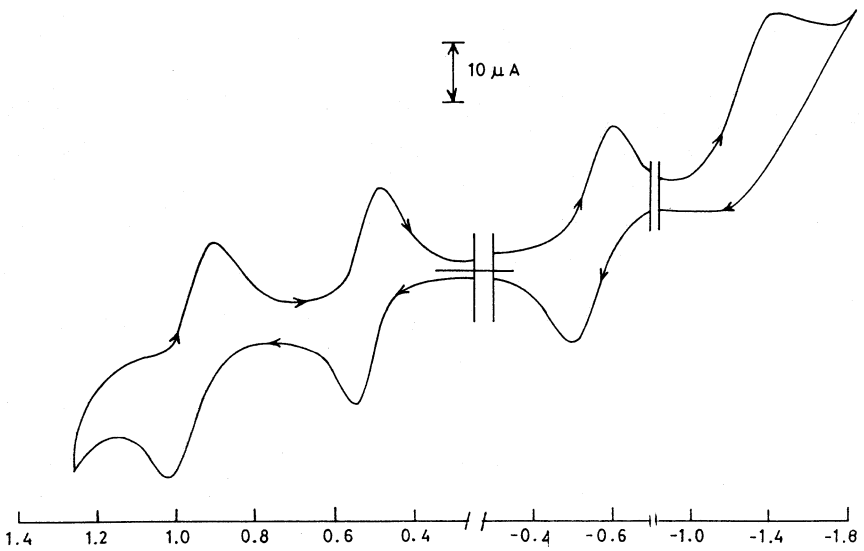

Fig. 4. Voltammogram of [Pt(*p*-tap)(tbcat)] in MeCN using a GC working electrode (SCE reference) at 298 K.

arylazopyridine ring by appropriate substitutent(s) in the respective rings. [Pt(aap)(*O*,*O*)] exhibit catechol/semiquinone and semiquinone/quinone oxidations and azo reductions during cyclic voltammetric studies. The reversibility of the catechol/semiquinone oxidation couple is dependent on the electron influx in the catechol ring.

6. Supplementary material

Crystallographic data for the structural analysis have been deposited with the Cambridge Crystallographic Data Center, CCDC No. 14472 for compound **2a**. Copies of this information may be obtained free of charge from The Director, CCDC, 12 Union Road, Cambridge, CB2 1EZ, UK (fax: +44-1223-336-033; e-mail: deposit@ccdc.cam.ac.uk or www: http://www.ccdc.cam.ac.uk).

Acknowledgements

We are thankful to the University Grants Commission (under the DSA scheme) and the Council of Scientific and Industrial Research, New Delhi for financial

help. GKR is grateful to Professor B.R. De, Vidyasagar University, Midnapore and Dr M. Banerjee, Burdwan University, Burdwan for their help.

References

[1] C. Handrosch, R. Dinnebier, G. Bondarenko, E. Bothe, F. Heinemann, H. Kisch, Eur. J. Inorg. Chem. (1999) 1259.
[2] F.R. Keene, Coord. Chem. Rev. 166 (1997) 121.
[3] B.K. Ghosh, A. Chakravorty, Coord. Chem. Rev. 95 (1989) 239.
[4] G.K. Lahiri, S. Bhattacharya, S. Goswami, A. Chakravorty, J. Chem. Soc., Dalton Trans. (1990) 561.
[5] N. Bag, A. Pramanik, G.K. Lahiri, A. Chakravorty, Inorg. Chem. 31 (1992) 40.
[6] C.K. Pal, S. Chattopadhyay, C. Sinha, D. Bandyopadhyay, A. Chakravorty, Polyhedron 13 (1994) 999.
[7] J. Chakravorty, S. Bhattacharya, Transition Met. Chem. 20 (1995) 138.
[8] R. Roy, P. Chattopadhyay, C. Sinha, S. Chattopadhyay, Polyhedron 15 (1996) 3361.
[9] B.K. Santra, G.A. Thakur, P. Ghosh, A. Pramanik, G.K. Lahiri, Inorg. Chem. 35 (1996) 3050.
[10] K.N. Mitra, S. Chaudhury, S. Goswami, S.M. Peng, Polyhedron 16 (1997) 1605.
[11] (a) M. Shivakumar, K. Pramanik, P. Ghosh, A. Chakravorty, Inorg. Chem. 37 (1998) 5968. (b) M. Shivakumar, K. Pramanik, P. Ghosh, A. Chakravorty, Chem. Commun. (1998) 2103.
[12] A.K. Ghosh, P. Majumder, L.R. Falvellow, G. Mostafa, S. Goswami, Organometallics 18 (1999) 5086.
[13] P. Majumder, S. Goswami, S.M Peng, Polyhedron 18 (1999) 2543.
[14] B.K. Santra, P. Munshi, G. Das, P Bharadwaj, K. Lahiri, Polyhedron 18 (1999) 617.
[15] B.S. Raghvendra, A. Kravorty, Ind. J. Chem., Sect. A 14 (1976) 166.
[16] D. Dutta, A. Chakravorty, Inorg. Chem. 22 (1983) 1085.
[17] B.K. Santra, G.K. Lahiri, J. Chem. Soc., Dalton Trans. (1997) 1883.
[18] A. Bharath, B.K. Santra, P. Munsi, G.K. Lahiri, J. Chem. Soc., Dalton Trans. (1998) 2643.
[19] T.K. Misra, D. Das, C. Sinha, P. Ghosh, C.K. Pal, Inorg. Chem. 37 (1998) 1672.
[20] P.K. Santra, T.K. Misra, D. Das, C. Sinha, A.M.Z. Slawin, J.D. Woollins, Polyhedron 18 (1999) 2869.
[21] S.J. Brown, S.C. Chow, S.J. Lippard, in: R.B. King (Ed.), Encyclopedia of Inorganic Chemistry, Wiley, New York, 1994, pp. 3305–3315.
[22] P.M. Takahara, C.A. Fredrick, S.J. Lippard, J. Am. Chem. Soc. 118 (1996) 12309.
[23] D. Das, C. Sinha, Transition Met. Chem. 23 (1998) 517.
[24] V. Anbalagan, T.S. Srivastava, Polyhedron 13 (1994) 291.
[25] O. Gandolfi, G. Dolcetti, M. Cais, Inorg. Chem. 19 (1980) 1785.
[26] C.A. McAuliffe, H.L. Sharma, N.D. Tinker, Studies in Inorganic Chemistry II: Chemistry of the Platinum Group Metals Recent Developments, Elsevier, Amsterdam, 1991, p. 571.
[27] C.G. Pierpont, R.M. Buchanan, Coord. Chem. Rev. 38 (1981) 45.
[28] G. Wilkinson (Ed.), Comprehensive Coordination Chemistry, vol. 5, Pergamon, Oxford, 1987.
[29] S.E. Livingstone, Synth. React. Inorg. Met. Org. Chem. 1 (1971) 1.
[30] C. Sinha, Ph.D. Thesis, Jadavpur University, India, 1990.
[31] A. Seal, S. Roy, Acta Crystallogr., Sect. C, Struct. Commun. 40 (1984) 929.
[32] F.A. Cotton, G. Wilkinson, Advanced Inorganic Chemistry, 3, Wiley, NewYork, 1972.
[33] D.J. Gordon, R.F. Fenske, Inorg. Chem. 21 (1982) 1785.
[34] S.B. Kumar, M. Chaudhury, J. Chem. Soc., Dalton Trans. (1991) 2169.